

MELITTIN – INDUCED CHANGES IN LIPID BILAYERS: A MOLECULAR ACOUSTIC STUDY

Linus N. Okoro

Department of Petroleum Chemistry and Engineering
American University of Nigeria, Yola, Nigeria

ABSTRACT

The effect of melittin at mole fractions of up to 3.75 mol%, on the dynamic and mechanical properties of 1,2-dipalmitoyl-*sn*-glycero-3-phosphatidylcholine (DPPC) was investigated using ultrasound velocimetry and densitometry. The isothermal compressibility and volume fluctuations of DPPC – melittin bilayer membrane in their different transition phases were determined. At the melting temperature, T_m , a general increase in velocity number $[u]$ as compared to the pure lipid was noticed. However, at 3.75 mol%, melittin displays the broadest peak and lowest value of $[u]$ compared to the other melittin concentrations, which could be linked to the lytic property of melittin at high peptide concentrations. The melittin concentration effects on the partial specific volume, v^o and the adiabatic compressibility coefficient of the lipid, β_S^{lipid} of the DPPC bilayer reveals a slight shift of the main transition to lower temperature and a continuous decrease in v^o with concentration increase above the T_m (except between 1 and 1.25%), as well as a decrease in β_S^{lipid} with decrease in melittin concentration. Again, the isothermal compressibility peak at the main transition drops drastically upon addition of melittin at concentrations as low as 1 mol% and then increases with increase in melittin concentration. At all melittin concentrations, β_T^{lipid} is greater than β_S^{lipid} in the gel-fluid region by ~ 20%. The maximum value of the relative volume fluctuations of 12 % is reached for DPPC at the main transition, and is strongly dampened upon addition of melittin. Only a slight decrease in the calculated relative volume fluctuations with melittin concentration is observed between concentrations 0 and 1.0 mol%.

Keywords: DPPC, Melittin, phospholipid ultrasound velocimetry, densitometry.

INTRODUCTION

Melittin, the principal toxic component in the venom of the European honeybee, *Apis mellifera*, is a cationic hemolytic peptide (Sessa *et al.*, 1969; Habermann, 1972; Tosteson *et al.* 1985). It constitutes 50% of the dry weight of the bee venom. The active peptide melittin is released from its precursor, promelittin, during its biosynthesis in honey bee and later gets formylated (Habermann, 1972). It is composed of 26 amino acids (NH₂-G-I-G-A-V-L-K-V-L-T-T-G-L-P-A-L-I-S-W-I-K-R-K-R-Q-Q-CONH₂) in which the amino-terminal region (residues 1–20) is predominantly hydrophobic whereas the carboxy-terminal region (residues 21–26) is hydrophilic due to the presence of a stretch of positively charged amino acids. Melittin amphiphilic property makes it water soluble and yet it spontaneously associates with both natural and artificial membranes (Dempsey, 1990). The crystal structures of melittin have been resolved by X-ray crystallography (Terwilliger *et al.*, 1982). In an aqueous solution of high peptide concentration, high pH value, or high ionic strength, tetrameric melittin of high symmetry is formed readily (Dempsey, 1990). The hydrophobic surface of each amphipathic α -helical monomer is essentially completely removed from solvent exposure upon tetramerization.

Melittin has been a source of inspiration for the development of novel antiviral and antibacterial agents that act at the membrane level to cause leakage in their lethal mechanism (Baghian *et al.*, 1997). Melittin causes bilayer micellization and membrane fusion and has also been observed to form voltage-dependent ion channels across planar lipid bilayers (Bechinger, 1997; Monette and Lafleur, 1996). The characteristic action of melittin is its hemolytic activity (Habermann, 1972; DeGrado *et al.*, 1982; Rudenko, 1995; Raghuraman and Chattopadhyay, 2005). It is commonly believed that multimeric pore formation is the mode of action of many naturally produced peptides such as antimicrobial peptides and toxins (Allende *et al.*, 2005; Rapaport *et al.*, 1996; Rex, 1996). Few studies have been attempted to monitor the structure and function of such pores and their results show that melittin forms pores that have a rather wide distribution of sizes. For example, the sizes of the melittin pores that are characterized by the inner pore diameter have been reported to be in the range of 10–60 Å, 13–24 Å and 25–30 Å (Rex, 1996; Matsuzaki *et al.*, 1997) from vesicle leakage experiments. The diameter of these pores is expected to increase when the peptide concentration is increased.

Under certain conditions, melittin molecules insert into the lipid bilayer and form multiple aggregated forms that

*Corresponding author email: Linus.okoro@aun.edu.ng

are controlled by temperature, pH, ionic strength, lipid composition and the lipid-to-peptide ratio. Lipid composition and phase separation appears to play a critical role in melittin-induced pore formation. The action of melittin on membrane proteins has been studied and apart from its ability to disrupt lipid bilayers, melittin affects the dynamics of membrane proteins. For instance, it has been shown that lytic concentrations of melittin dramatically reduce the rotational mobility of band 3 protein in human erythrocyte membranes (Clague and Cherry, 1988; Hui *et al.*, 1990).

Melittin oligomers appear to be involved in membrane permeabilization, which supralinearly depends on the peptide concentration in both voltage-gated ion channel experiments (Pawlak *et al.*, 1991). The orientation of melittin in a phospholipid bilayer has been explored (including molecular dynamics simulation studies) and was found to be sensitive to the experimental conditions (Bachar and Becker, 2000; Bradshaw *et al.*, 1994; Lin and Baumgaertner, 2000). The aggregation state of melittin in membranes is an important issue since this property is presumed to be associated with the function of melittin. This can be appreciated by the fact that melittin forms voltage-gated channels (Tosteson, 1981) which may require self association of melittin monomers to form pores in membranes. It is not known whether pore-forming melittin aggregates pre-exist in the membrane in the absence of an applied membrane potential.

Light scattering and ^{31}P -NMR have been used to monitor the effects of melittin on phosphatidylcholine (PC) bilayers of variable acyl chain length (from C16:0 to C20:0). From the experiment it was observed that melittin interacts with all lipids provided the interaction is initiated in the lipid fluid phase (Faucon *et al.*, 1995). Unger *et al.* (2001) has studied the effect of cyclization of melittin analogues on the structure, function, and model membrane interactions. It was found that cyclization altered the binding of melittin analogues to phospholipid membranes and had increased the antibacterial activity but decreased the hemolytic activity. The interaction of melittin and phospholipids has been extensively studied partly because it has a secondary amphiphilic property (Terwilliger *et al.*, 1982; Ladokhin and White, 1999) as well as a model for this class of peptides. Interestingly, the role of melittin–lipid interactions has also been shown to be responsible, along with more specific binding of melittin with membrane proteins, for the inhibition of the Ca^{2+} -ATPase (Baker *et al.*, 1995) and protein kinase C (Raynor *et al.*, 1991). The dependence of melittin aggregation on temperature (Iwadate *et al.*, 1998) and its thermodynamics, as determined by circular dichroism spectroscopy, has been reported (Wilcox and Eisenberg, 1992).

The interaction of melittin with membranes in general, and with cholesterol-containing membranes in particular has been explored, with possible relevance to its interaction with the erythrocyte membrane (Raghuraman and Chattopadhyay, 2004). In an experiment to investigate the lipid-binding behavior of three peptides: melittin, magainin II, and cecropin P1, Lad *et al.* observed that melittin binding to lipids was 50% greater for either magainin or cecropin (Lad *et al.*, 2007).

The lytic activity of melittin has been reported to strongly depend on the membrane composition. Whereas zwitterionic lipids are more affected by the melittin lytic activity (Monette and Lafleur, 1995), membranes with longer hydrocarbon chains are less affected (Bradrick *et al.*, 1995). Although cell lysis by melittin has been extensively studied, the molecular mechanism of its hemolytic activity is still not well understood. In particular, the role of specific lipids on melittin-induced hemolysis is not yet clear. Detailed mechanical properties and thermodynamic information on melittin in membranes is important due to the widespread occurrence of the motif in host-defense peptides and membrane proteins. DPPC, one of the best studied phospholipids is a zwitterionic phospholipid with a medium tail consisting of 16 carbons and has a length appropriate for the study of melittin action on lipids.

In the present study, a more detailed dynamic and mechanical picture of melittin-DPPC bilayers around the phase transition temperature as revealed by ultrasound velocimetry and densitometry is obtained, and to gain more insight into the molecular mechanism of the lytic and fusion activity of melittin on DPPC membranes.

MATERIALS AND METHODS

Liposome Preparation

1,2-Dipalmitoyl-3-*sn*-phosphatidylcholine (DPPC) was purchased from Avanti Polar Lipids (Alabaster, AL, USA), while Melittin ($\geq 97\%$ purity) as a lyophilized solid was obtained from Calbiochem (Germany). Both were used without further purification. Multilamellar vesicles (MLV) of DPPC and melittin with designated mole ratios were mixed in chloroform-methanol mixture (3:1 v/v) and dried as a thin film under a stream of nitrogen and then freeze-dried in a freeze-dryer (Christ, Osterode, Germany) under high vacuum overnight. The lipid films were hydrated in a Tris buffer (10 mM Tris-HCl, 100 mM NaCl, pH 7.4), followed by vortexing at $\sim 60^\circ\text{C}$ (above the main phase transition temperature, T_m , of DPPC ($\sim 41.5^\circ\text{C}$ (Cevc and Marsh, 1987; Okoro and Winter, 2008) and five freeze-thaw cycles, resulting in homogeneous multilamellar vesicles (MLVs). Large unilamellar vesicles (LUVs) of uniform shape and size used in the ultrasound velocity and the density measurements were prepared from the MLVs by extrusion (MacDonald *et al.*, 1991)

using a Mini-Extruder (Avanti Polar Lipids Inc., USA), and passing them through 100nm Nuclepore® Polycarbonate Track-Etch™ Membranes (Whatman GmbH, Dassel, Germany) at ~60°C. The final DPPC concentration used in the ultrasound velocity and the density measurements for melittin was 5mg/mL.

Ultrasound velocity and density measurements

The ultrasound velocity u of the vesicles was determined simultaneously using a differential ultrasonic resonator device ResoScan (TF Instruments, Heidelberg, Germany, operating in a frequency range of 7.2 – 8.5 MHz. (Eggers and Kustin, 1969; Eggers and Funk, 1973; Stuehr and Yeager, 1965).

Ultrasonic measurements are extremely sensitive to temperature changes. Reproducibility and accuracy is therefore crucially dependent on TFI's Ultra-high Precision Peltier-Thermostat that reaches temperature constancy better than 1 mK (0,001°C), and features a fast heating, cooling and equilibration time between 5 and 85°C.

The sound velocity of the lipid dispersion was determined relative to that in the buffer solution at the same temperature in terms of the velocity number, $[u]$, defined as (Stuehr and Yeager, 1965).

$$[u] = (u - u_0) / u_0 \quad (1)$$

Where u and u_0 denote the sound velocity in the solution and in the solvent, respectively, and c is the solute concentration in mol/L.

The densities, ρ and ρ_0 , of the lipid solution and the solvent, respectively were measured by a high-precision density meter DMA 5000 (Anton Paar, Graz, Austria) based on the mechanical oscillator principle (Kratky *et al.*, 1973), corrected for viscosity-induced errors.

The partial molar volume, V^0 , of the lipid is evaluated from the density data by the given relation:

$$V^0 = \left(\frac{\partial V}{\partial n} \right) \cong \frac{M}{\rho_0} - \frac{\rho - \rho_0}{\rho_0 c} \quad (2)$$

Where V is the volume, n the number of solute molecules in moles, and M is the molar mass of the solute. The very right term is valid only for diluted lipid suspensions as used in this study.

The adiabatic compressibility coefficient, $\beta_S = -1/V (\partial V / \partial p)_S$ (V , p and S are the volume, the pressure and entropy, respectively), the speed of sound propagation, u , in the medium, and the density, ρ are related by the expression:

$$\beta_S = 1 / u^2 \rho \quad (3)$$

In molecular acoustics, due to the additivity of all components of the system, the partial molar adiabatic compressibility, K_S^0 , is generally used, which is given by;

$$K_S^0 = \left(\frac{\partial K_S}{\partial n} \right) = \left(\frac{\partial V^0}{\partial p} \right)_S \cong \beta_{S,0} \left(2(V^0 - [u]) - \frac{M}{\rho_0} \right), \quad (4)$$

where $K_S = \beta_S V$ is the adiabatic compressibility and $\beta_{S,0}$ is the adiabatic compressibility coefficient of the solvent. By dividing the partial molar quantities V^0 and K_S^0 by the molar mass of the solute we obtain the partial specific values, i.e., the partial specific volume, v^0 , and the partial specific adiabatic compressibility, k_S^0 . Accordingly, the concentration, c , in Eq. 1 becomes c/M , which is then expressed in mg/mL.

The sound velocity was determined with a relative error better than 10^{-3} %, corresponding to a precision higher than 5×10^{-5} mL/g in $[u]$. The density values were measured with relative error smaller than 10^{-3} %, so the accuracy in v^0 is better than 10^{-4} mL/g. Therefore, considering the relative errors of $[u]$ and v^0 , the certainty in k_S^0 taken from Eq. 4 is within 10^{-12} mL/gPa. In both methods, the corresponding values were measured at discrete temperatures (read with an accuracy of 10^{-3} °C), resulting in an average temperature scan rate of ~12 °C/h.

The adiabatic compressibility of the lipids, β_S^{lipid} , is defined as

$$\beta_S^{\text{lipid}} = -\frac{1}{v^0} \left(\frac{\partial v^0}{\partial p} \right)_S \quad (5)$$

which is related to the partial specific adiabatic compressibility, k_S^0 , by

$$k_S^0 = v^0 \beta_S^{\text{lipid}} \quad (6)$$

β_S^{lipid} can thus be directly obtained from combined ultrasound velocity and density measurements.

Lipid bilayer thermotropic main phase transitions are considered to be of weak first-order, i.e., they show typical features of first-order phase transitions, such as abrupt changes in specific volume or a peak in the enthalpy and entropy, but also significant fluctuations in volume and lamellar d -spacing, which are typical for a second-order phase transition. The isothermal compressibility, K_T , is directly proportional to the volume fluctuations of the system (Wilson, 1957; Hill, 1960). In a system exhibiting a first-order transition, K_T diverges at the phase transition temperature, whereas it exhibits a power-law behavior ($K_T \propto |T - T_d|^{-\gamma}$), with a particular critical exponent ($\gamma = 1.24$ for 3D systems) in the critical-point region of a second-order phase transition (Stanley,

1971; Winter *et al.*, 1999). By the ultrasound velocity and the density measurements, however, only the adiabatic compressibility, K_S , can be determined (see Eqn. 3 and 4). The isothermal compressibility can be calculated from (Hill, 1960)

$$K_T = K_S \frac{C_p}{C_V} \quad (7)$$

where C_p and C_V are the heat capacities at constant pressure and volume, respectively, which, using Maxwell relations, can also be expressed as

$$K_T = K_S + \frac{T}{C_p} \left(\frac{\partial V}{\partial T} \right)_p^2 = K_S + \frac{TE^2}{C_p} \quad (8)$$

with the thermal expansion $E = (\partial V / \partial T)_p$. Hence, the isothermal compressibility can be obtained from the adiabatic one when the thermal expansion and the heat capacity data are available. Differentiating Eqn. 8 yields the exact differential of K_T , dK_T , which is given as:

$$dK_T = dK_S + \frac{E^2}{C_p} dT + 2 \frac{TE}{C_p} dE - \frac{TE^2}{C_p^2} dC_p \quad (9)$$

For convenience, Eqn. 8 is adapted through Eqn. 9 by thermodynamic treatment to a form where the corresponding partial specific quantities are taken (Chalikian, 2003):

$$k_T^o = k_S^o + \frac{T\alpha_0^2}{\rho_0 c_{p,0}} \left(2 \frac{e^o}{\alpha_0} - \frac{C_p^o}{\rho_0 c_{p,0}} \right) \quad (10)$$

k_T^o is the partial specific isothermal compressibility, α_0 ($\alpha = E/V$) and $c_{p,0}$ are the thermal expansion coefficient and the specific heat capacity of the solvent, respectively; e^o and C_p^o are the partial specific expansivity and the partial specific heat capacity of the lipid, respectively; the latter is given by (Privalov, 1980)

$$C_p^o = \frac{\Delta C_p}{m} + \frac{v^o}{v_0^o} c_{p,0} \quad (11)$$

where m is the mass of the solute.

The corresponding isothermal compressibility of the lipid, $\beta_T^{\text{lipid}} = k_T^o / v^o$ (note that β_T^{lipid} differs from the partial specific isothermal compressibility coefficient, β_T^o , which is defined as $\beta_T^o = 1/M (\partial \beta_T / \partial n) = \beta_T v^o / V$), can be obtained from Eqn. 10 and is given as:

$$\beta_T^{\text{lipid}} = \beta_S^{\text{lipid}} + \frac{T\alpha_0^2}{v^o \rho_0 c_{p,0}} \left(2 \frac{e^o}{\alpha_0} - \frac{C_p^o}{\rho_0 c_{p,0}} \right) \quad (12)$$

For simplification, we denote in Eqn. 12 the second and third term as β_e^{lipid} , and β_C^{lipid} , respectively:

$$\beta_T^{\text{lipid}} = \beta_S^{\text{lipid}} + \beta_e^{\text{lipid}} - \beta_C^{\text{lipid}} \quad (13)$$

Hence, the isothermal compressibility coefficient, β_T^{lipid} , is given as a sum of the adiabatic compressibility, β_S^{lipid} , an expansion term, β_e^{lipid} , and a heat capacity term, β_C^{lipid} . Interestingly, as can be seen from Eqs. 10 and 12, the heat capacity term has a compensating effect, balancing that of the thermal expansion on the adiabatic compressibility.

The thermodynamic parameters C_p , K_T and E are directly related to corresponding fluctuation parameters (Cooper, 1984): i) the square average of the enthalpy fluctuations, its variance, $\langle \Delta H^2 \rangle$, is determined by the heat capacity, C_p , of the system, ii) the square average of the volume fluctuations $\langle \Delta V^2 \rangle$ as given by the respective isothermal compressibility, K_T , and iii) the covariance between H and V , $\langle \Delta H \Delta V \rangle$, is related to the thermal expansion, E :

$$\langle \Delta H^2 \rangle = RT^2 C_p \quad (14a)$$

$$\langle \Delta V^2 \rangle = RT K_T \quad (14b)$$

$$\langle \Delta H \Delta V \rangle = RT^2 E = RT^2 V \alpha \quad (14c)$$

As seen from Eqn. 14c, the thermal expansion couples contributions from the heat capacity and the isothermal compressibility.

RESULTS AND DISCUSSION

Sound velocimetry and densitometry are sensitive tools to study the mechanics and thermodynamics of biomolecules and biocolloids. When the two methods are used simultaneously to study the phase transition peculiarities of lipid bilayer, they enable one to determine the degree of phase transition cooperativity. This advantage is most useful in the study protein / peptide-lipid interactions, since the determination of mechanical parameters is crucial for an evaluation of the size of distorted membrane structure around proteins or peptides (Hianik and Passechnik, 1995). Ultrasound and densitometry techniques were used to measure the velocity number, $[u]$, and the partial specific volume, v^o , of the DPPC-melittin mixtures. From equation 4, the partial specific adiabatic compressibility, k_S^o , of the lipid dispersion was determined.

Figure 1a shows the temperature dependence of velocity number $[u]$ for the DPPC – melittin mixtures. Decrease of $[u]$ with rise in temperature is observed, leading to the typical anomalous dip (Mitaku *et al.*, 1978; Kharakoz *et al.*, 1993; Schrader *et al.*, 2002; Krivanek *et al.*, 2008) in the vicinity of T_m for pure lipids. The lowest value of $[u]$ at T_m is $\sim 0.15 \text{ mL/g}$ for pure DPPC, which is consistent with Mitaku and co-workers data (Mitaku *et al.*, 1978). It should be noted, however, that the size and the width of the dip in $[u]$ depends on the sample preparation Mitaku

et al. (1978), which is related to the different degree of cooperativity of the main phase transition, on the lipid concentration (Kharakoz *et al.*, 1993), and on the ultrasound frequency applied for the measurement itself (Mitaku and Data, 1982), which is related to the heat exchange within the period of the sound wave (Osdol *et al.*, 1989; Heimburg and Marsh, 1996). The dip in the ultrasonic number profiles will be more pronounced at lower frequencies, because C_p assumes higher values, leading to an increase of the adiabatic compressibility at lower frequencies. The frequency dependence of the ultrasonic absorption coefficient of DPPC suspensions has been measured. The excess absorption data has been described by a relaxation term with a discrete relaxation time, displaying some evidence of critical slowing down near the phase transition (Heimburg and Marsh, 1996).

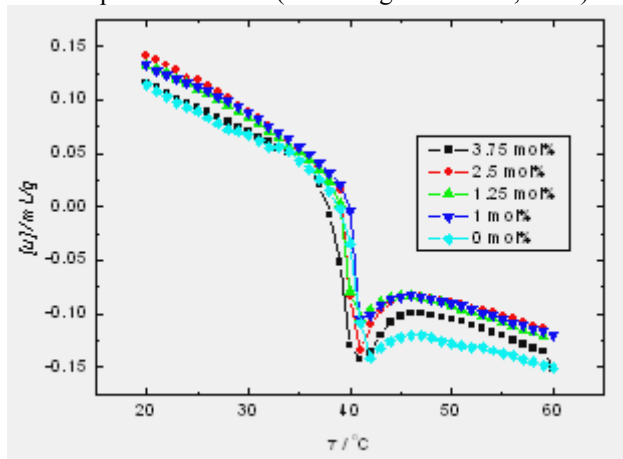


Fig. 1a. The temperature dependence of the ultrasound velocity number, $[u]$, for DPPC – melittin mixtures.

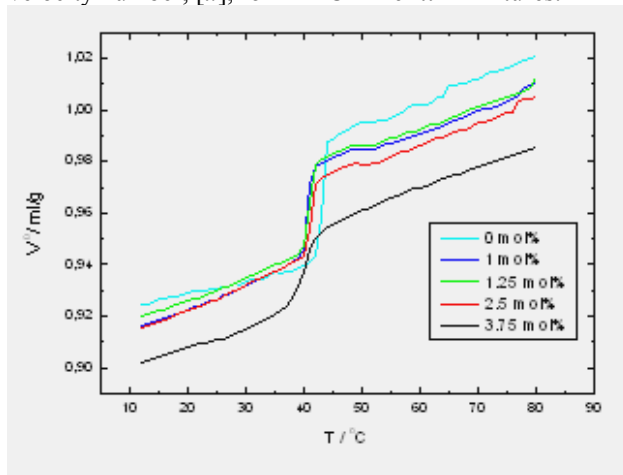


Fig. 1b. The temperature dependence of the partial specific volume, v^o , for DPPC – melittin mixtures.

Upon addition of melittin to DPPC, and at T_m , there is a general increase in $[u]$ as compared to the pure lipid. However, the sample with 3.75% melittin is observed to have the lowest value of $[u]$ compared to the lower melittin concentrations studied. It also exhibits the

broadest peak. The dip continues to increase with a decrease in melittin concentration, with the highest value being at 1.25% and 1% melittin. This is in contrast to the earlier studied systems lipid-gramicidin D and lipid-sterol systems (Krivanek *et al.*, 2008) and might be linked to the lytic property of melittin at higher concentrations, in particular in the lipid phase transition region.

Further observation is that pure DPPC has the least $[u]$ both in the gel phase and in the fluid phase region. The ultrasonic velocity profiles provide information about isothermal and adiabatic compressibilities and reveal the deep linkage between the different thermodynamic response functions.

In addition, for the DPPC-melittin mixture, both below the pre-transition and above the main transition, the sound velocity number is approximately the same for the concentrations 1, 1.25 and 2.5% melittin. Generally, addition of melittin to DPPC bilayers causes a slight shift of the melting phase transition to lower temperatures. The ultrasonic velocity profiles provide information about isothermal and adiabatic compressibilities and reveal the deep linkage between the different thermodynamic response functions.

The temperature dependence of the partial specific volume, v^o , as measured by the densitometer, is shown in figure 1b, and an increase of v^o with temperature is observed throughout the whole melting transition regime. A step-like change at the transition temperature T_m is observed for pure DPPC and for DPPC – melittin concentrations up to 2.5 mol%. As already stated above, the changes in $[u]$ and v^o with increase in melittin concentration are clearly observed in the T_m region, indicating increased volume fluctuations in this temperature region. The partial specific volume v^o is smaller both below and above T_m for the DPPC – melittin mixtures. A substantial decrease is observed for v^o upon addition of melittin up to 3.75 mol%, which could be attributed to the lytic property of melittin at high melittin concentrations. A more detailed behaviour of v^o in the gel phase (25°C) and in the fluid phase (55°C) is illustrated in figure 2.

Figure 3a displays the temperature dependent partial specific adiabatic compressibility, k_s^o , of the transitions of both pure DPPC and the DPPC – melittin mixtures, as determined from Equation 4. The k_s^o for pure DPPC has the highest value, increasing from 2.35 mL/gPa at 20°C and abruptly reaching 5.25 mL/gPa (55°C) at T_m , as expected. A slight drop occurs right after T_m , and k_s^o finally continues to increase with increasing temperature to reach the highest level of 5.4 mL/gPa at 60°C. Generally, a slight shift to lower temperatures for k_s^o in the melting transition region is observed, just as observed

in $[u](T)$. Significant broadening of the transition peak is observed at the 3.75 % concentration. The temperature dependence of β_S^{lipid} for the DPPC – melittin mixtures is displayed in Fig.3b and exhibits similar shape as $k_S^o(T)$ (Eqn.6).

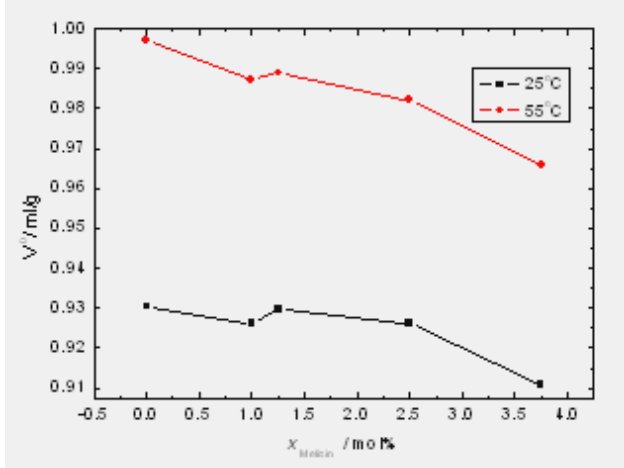


Fig. 2. The partial specific volume of DPPC-melittin mixtures as a function of melittin concentration at 25 and 55 °C.

At 20 and 60 °C, the β_S^{lipid} values are $3.0 \times 10^{-10} \text{ Pa}^{-1}$ and $5.4 \times 10^{-10} \text{ Pa}^{-1}$, respectively. The value for β_S^{lipid} of $3.4 \times 10^{-10} \text{ Pa}^{-1}$ at 30 °C is in good agreement with $\beta_S^{\text{lipid}} = 3.5 \times 10^{-10} \text{ Pa}^{-1}$ obtained by Mitaku and coworkers (Mitaku *et al.*, 1978). Just as for k_S^o , the anomalous increase of β_S^{lipid} around T_m is still significant at all melittin concentrations. The data for the adiabatic compressibility coefficient of the DPPC-melittin mixtures as a function of melittin concentration at 25 and 55 °C is summarized in figure 4. The plot reveals a gradual decrease in β_S^{lipid} with melittin concentration in both the gel (25°C) and the fluid

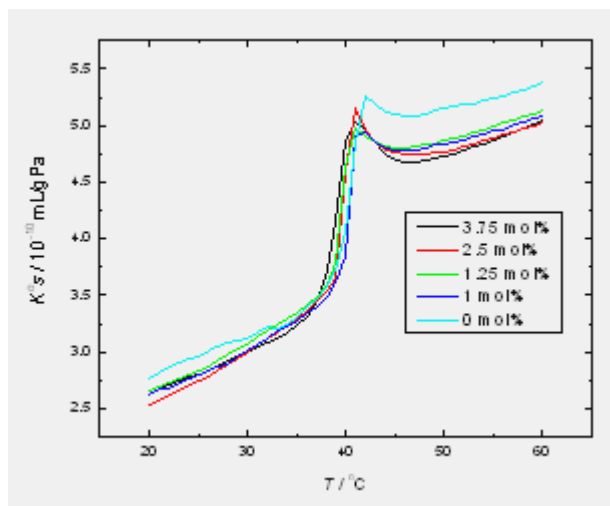


Fig. 3a. The temperature dependence of the partial specific adiabatic compressibility, k_S^o , of DPPC-melittin mixtures.

phase (55°C) up to 2.5 mol% melittin. An increase in β_S^{lipid} upon addition of 3.75mol% is observed, implying a disordering effect (which could be attributed to melittin pore formation) at these higher melittin concentrations.

Isothermal Compressibility and Volume fluctuations of DPPC – melittin mixtures

Figure 5 displays the temperature dependence of the isothermal compressibility coefficient of DPPC-melittin mixtures at different melittin concentrations. It was observed that the isothermal compressibility peak at the main transition drops drastically ($\sim 75\%$) upon addition of melittin at concentrations as low as 1 mol%. This decrease in β_T^{lipid} corresponds to a similar observed strong decrease (80%) of the thermal expansion coefficient in a differential scanning calorimetry (unpublished), again indicating the close relationship between the corresponding fluctuations ($\langle \Delta V^2 \rangle$ vs. $\langle \Delta H \Delta V \rangle$) (Krivanek *et al.*, 2008; Okoro and Winter, 2008). Furthermore, there was an increase in β_T^{lipid} with increase in melittin concentrations at the transition temperature (disordering effect at higher melittin concentrations). At all melittin concentrations, β_T^{lipid} is greater than β_S^{lipid} by $\sim 20\%$ in the whole temperature range covered.

Assuming that the partial specific volume, v_o , is largely determined by the lipid term (see Eqn. 2), i.e. v_o reflects the “real” volume of the lipid molecule, which allows us to modify Eq. 18 and to convey the relative volume fluctuations given as

$$\sqrt{\frac{\langle \Delta V^2 \rangle}{V^2}} = \sqrt{\frac{RT\beta_T^{\text{lipid}}}{Mv^o}} \quad (15)$$

The calculated temperature dependent relative volume

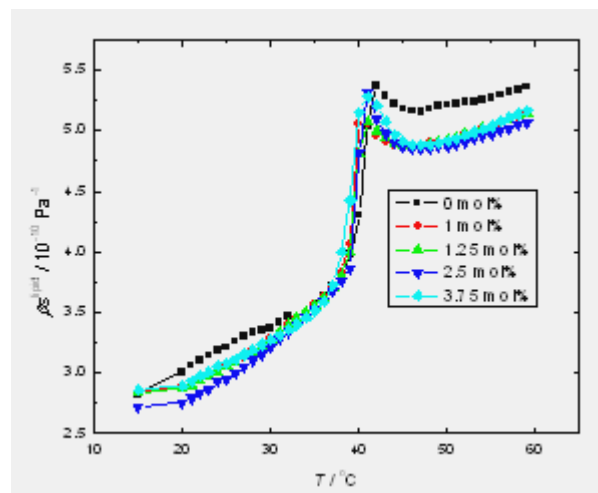


Fig. 3b. The temperature dependence of the adiabatic compressibility coefficient, β_S^{lipid} , of DPPC - melittin fractions.

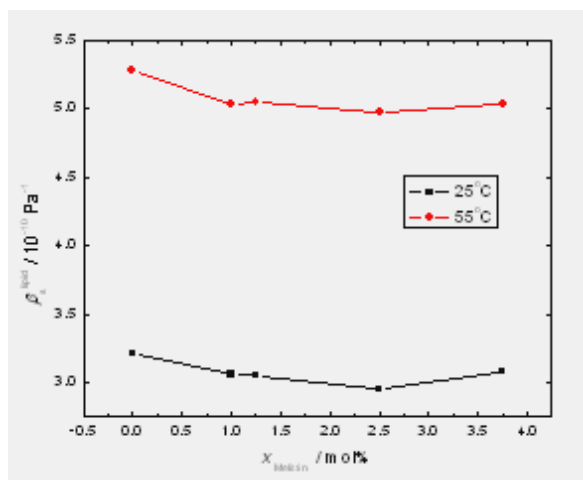


Fig. 4. The adiabatic compressibility coefficient of lipid data of DPPC-melittin mixtures as a function of melittin concentration at 25 and 55°C, respectively.

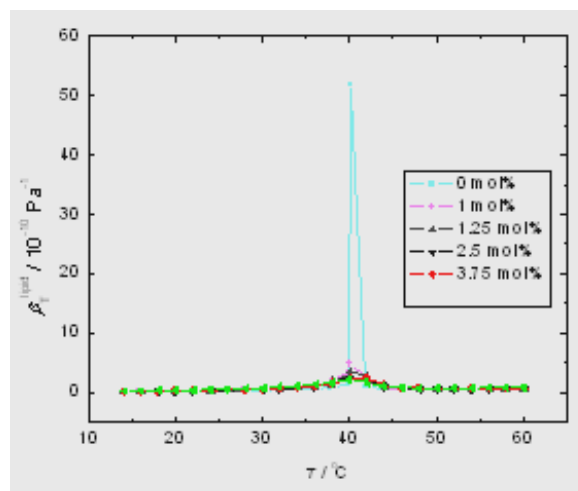


Fig. 5. The temperature dependence of the isothermal compressibility coefficient of the DPPC – melittin mixtures, β_T^{lipid} .

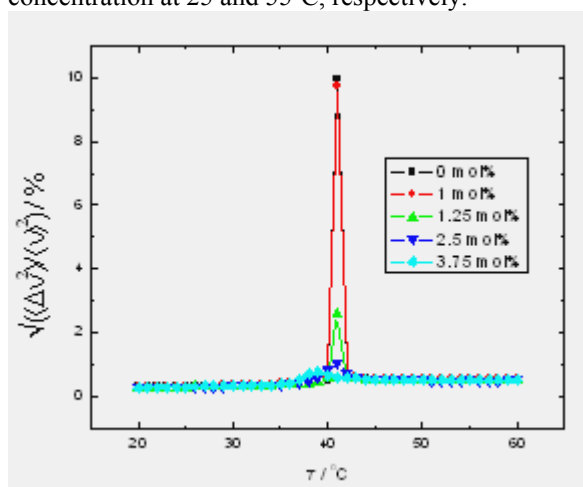


Fig. 6. The calculated relative volume fluctuations for DPPC-melittin mixtures at different melittin molar fractions x_m .

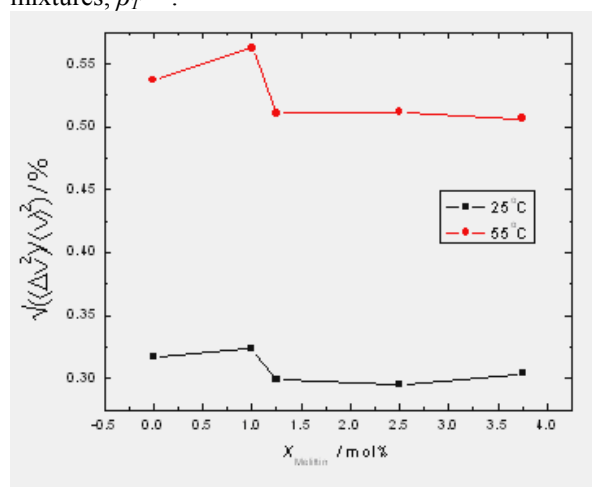


Fig. 7. The temperature dependence of the calculated relative volume fluctuations at 25 and 55°C for DPPC-melittin mixtures at different melittin mole fractions X_m .

fluctuations for DPPC-melittin mixtures are displayed in figure 6. Only a slight decrease in the calculated relative volume fluctuations with melittin concentration was observed between concentrations 0% and 1.0mol%. Above the main transition temperature, basically no change is observed in the temperature dependence of the calculated relative volume fluctuations (at 55°C) for DPPC-melittin concentrations of between 1.25 and 3.75mol% (Fig. 7).

CONCLUSION

In summary, the study has provided further insights into the disruptive effects of melittin on membrane bilayers. In this work, molecular acoustics (ultrasound velocity and densitometry) and calorimetry were used to determine isothermal compressibility and volume fluctuations of DPPC – melittin bilayer membranes in their different

phases. The study revealed a considerable influence of melittin on the thermodynamic, mechanical, and compressibility properties of DPPC bilayers. It is observed that fluctuations are maximal at the melting point, and that the compressibility is proportional to the local fluctuations in the volume. Oliynyk *et al.* (2007) have demonstrated that melittin incorporation to membranes lead to pore formation and the structure of the melittin pores depends on the thermodynamic state of the membrane. From their AFM images they concluded that at 1mol% melittin, transmembrane pores are induced in the gel phase of DPPC bilayers. Generally, the peptides in model and biological membranes can strongly affect the local state of the system, and the effect of peptide may also depend on the overall state of the membrane. Peptides like alamethicin tend to increase the permeability of biological membranes by not only forming water pores, but also by shifting the surrounding bilayer to more

disordered states which are more permeable for small molecules. Hence, the state of the membrane can be a regulating factor of the action of antibiotic peptides like melittin, influencing their capability to form transmembrane pores. At T_m , a general increase in $[u]$ as compared to the pure lipid is observed. However, the 3.75 % melittin induces the broadest peak and lowest value of $[u]$ compared to other melittin concentrations which could be due to changes of hydration of the membrane as a result of the binding process. The dip continued to increase with decrease in melittin concentration, with the highest value being at 1.25 and 1% melittin. The melittin concentration effects on v^o and β_S^{lipid} of the bilayer reveals a slight shift of the main transition to lower temperature and a continuous decrease in v^o (within the range of concentrations studied) above the T_m with concentration (except between 1 and 1.25%), as well as a decrease in β_S^{lipid} with decrease in melittin concentration. Furthermore, the isothermal compressibility peak at the main transition drops drastically upon addition of melittin at concentrations as low as 1 mol% and then increases with increase in melittin concentration. In addition, it was found that at all melittin concentrations β_T^{lipid} is greater than β_S^{lipid} in the gel-fluid region by $\sim 20\%$. The maximum value of the relative volume fluctuations of 12% is reached for DPPC at the main transition, and is strongly dampened upon addition of melittin. Only a slight decrease in the calculated relative volume fluctuations with melittin concentration is observed between concentrations 0 and 1.0 mol%.

ACKNOWLEDGEMENT

Grateful to Prof. Dr. R. Winter, Department of Physical Chemistry, Dortmund University of Technology, Germany, in whose laboratory this work was carried out. Krivanek useful discussion is appreciated. Financial support from the Deutsche Forschungsgemeinschaft (DFG), and the regional country Northrhine Westfalia is gratefully acknowledged.

REFERENCES

- Allende, D., Simon, SA. and McIntosh, TJ. 2005. Melittin-induced bilayer leakage depends on lipid material properties: evidence for toroidal pores. *Biophys. J.* 88:1828-1837.
- Bachar, M. and Becker, O. 2000. Protein-induced membrane disorder: A molecular dynamics study of melittin in a dipalmitoylphosphatidylcholine Bilayer. *Biophys. J.* 78:1359-1375.
- Baghian, A., Jaynes, J., Enright, F. and Kousoulas, K. 1997. An amphipatic α -helical synthetic peptide analogue of melittin inhibits herpes simplex virus-1 (HSV-1)-induced cell fusion and virus spread. *Peptides.* 18:177-183.
- Baker, KJ., East, JM. and Lee, AG. 1995. Mechanism of inhibition of the Ca²⁺-ATPase by melittin. *Biochemistry.* 34:3596-3604.
- Bechinger, B. 1997. Structure and functions of channel-forming peptides: Magainins, cecropins, melittin and alamethicin. *J. Membr. Biol.* 156:197-211.
- Bradrick, TD., Philippetis, A. and Georghiou, S. 1995. Stopped-flow fluorometric study of the interaction of melittin with phospholipid bilayers: Importance of the physical state of the bilayer and the acyl chain length. *Biophys. J.* 69:1999-2010.
- Bradshaw, JP., Dempsey, CE. and Watts, A. 1994. A combined x-ray and neutron diffraction study of selectively deuterated melittin in phospholipid bilayers: Effect of pH. *Mol. Membr. Biol.* 11:79-86.
- Cevc, G. and Marsh, D. 1987. *Phospholipid Bilayers.* John Wiley and Sons, New York, USA.
- Chalikian, TV. 2003. Volumetric Properties of Proteins. *Annu. Rev. Biophys. Biomol. Struct.* 32:207-235.
- Clague, MJ. and Cherry, RJ. 1988. Comparison of p25 presequence peptide and melittin. Red blood cell haemolysis and band 3 aggregation. *Biochem J.* 252:791-794.
- Cooper, A. 1984. Protein fluctuations and the thermodynamic uncertainty principle. *Prog. Biophys. Molec. Biol.* 44:181-214.
- DeGrado, WF., Musso, GF., Lieber, M., Kaiser, ET. and Kezdy, FJ. 1982. Kinetics and mechanism of hemolysis induced by melittin and by a synthetic melittin analogue. *Biophys. J.* 37:329-338.
- Dempsey, CE. 1990. The actions of melittin on membranes. *Biochim. Biophys. Acta.* 1031:143-161.
- Eggers, F. and Kustin, K. 1969. Ultrasonic methods. *Methods Enzymol.* 16:55-80.
- Eggers, F. and Funk, T. 1973. Ultrasonic measurements with millilitre liquid sample in the 0.5 – 100 MHz range. *Rev. Sci. Instr.* 44:969-978.
- Faucon, J-F., Bonmatin, J-M., Dufourcq, J. and Dufourc, E. 1995. Acyl chain length dependence in the stability of melittin-phosphatidylcholine complexes. A light scattering and 31P-NMR study. *Biochim. Biophys. Acta.* 1234:235-243.
- Habermann, E. 1972. Bee and wasp venoms. *Science.* 177:314-322.
- Heimburg, T. and Marsh, D. 1996. Thermodynamics of the interaction of proteins with lipid membranes. In: *Biological Membranes: A Molecular Perspective from Computation and Experiment.* Eds. Merz, KM. and Roux, B. Birkhauser, Boston. 405-462.

- Hianik, T. and Passechnik, VI. 1995. *Bilayer Lipid Membranes: Structure and Mechanical Properties*, Kluwer Academic, Dordrecht/ Boston/London.
- Hill, TL. 1960. *An Introduction to Statistical Thermodynamics*. Dover, New York, USA.
- Hui, SW., Stewart, CM. and Cherry, RJ. 1990. Electron microscopic observation of the aggregation of membrane proteins in human erythrocyte by melittin. *Biochim Biophys. Acta.* 1023:335-340.
- Iwadate, M., Asakura, T. and Williamson, MP. 1998. The structure of the melittin tetramer at different temperatures. An NOE-based calculation with chemical shift refinement. *Eur J. Biochem.* 257:479-487.
- Kharakoz, DP., Colotto, A., Loher, K. and Laggner, P. 1993. Fluid-gel interphase line tension and density fluctuations in dipalmitoylphosphatidylcholine multilamellar vesicles: an ultrasonic study. *J. Phys. Chem.* 97:9844-9851.
- Kratky, O., Leopold, H. and Stabinger, H. 1973. The determination of partial specific volume of protein by the mechanical oscillator technique. *Methods Enzymol.* 27:98-110.
- Krivanek, R., Rybar, P., Prenner, EJ. and McElhaney, RE. 2001. Interaction of the antimicrobial peptide gramicidin S with dimyristoyl-phosphatidyl choline bilayer membranes: A densitometry and sound velocimetry study *Biochim. Biophys Acta.* 1510:452-463.
- Krivanek, R., Okoro, L. and Winter, R. 2008. Effect of cholesterol and ergosterol on the compressibility and volume fluctuations of phospholipid-sterol bilayers in the critical point region – A molecular acoustic and calorimetric study. *Biophys. J.* 94:3538-3548.
- Lad, M., Birembaut, F., Clifton, L., Frazier, R., Webster, J. and Green, R. 2007. Antimicrobial Peptide-Lipid Binding Interactions and Binding Selectivity. *Biophys. J.* 92:3575-3586.
- Ladokhin, A. and White, S. 1999. Folding of amphiphilic α -helices on membranes: Energetics of helix formation by melittin. *J. Mol. Biol.* 285:1363-1369.
- Lin, J-H. and Baumgaertner, A. 2000. Stability of a Melittin Pore in a Lipid Bilayer: A Molecular Dynamics Study. *Biophys. J.* 78:1714-1724.
- MacDonald, RC., MacDonald, RI., Menco, BP., Takeshita, K., Subbarao, NK. and Hu, LR. 1991. Small-volume extrusion apparatus for preparation of large unilamellar vesicles. *Biochim. Biophys. Acta.* 1061:297-303.
- Matsuzaki, K., Yoneyama, S. and Miyajima, K. 1997. Pore formation and translocation of melittin. *Biophys. J.* 73:831-838.
- Mitaku, S., Ikegami, A. and Sakanishi, A. 1978. Ultrasonic studies of lipid bilayer phase transition in synthetic phosphatidylcholine liposomes. *Biophys. Chem.* 8:295-304.
- Mitaku, S. and Data, T. 1982. Anomalies of nanosecond ultrasonic relaxation in the lipid bilayer transition. *Biophys. Biochim. Acta.* 688:411-421.
- Monette, M. and Lafleur, M. 1996. Influence of lipid chain unsaturation on melittin-induced micellization. *Biophys. J.* 70:2195-2202.
- Okoro, L. and Winter, R. 2008. Pressure Perturbation Calorimetric Studies on Phospholipid-Sterol Mixtures. *Z. Naturforsch.* 63b:769-778.
- Oliynyk, V., Kaatz, U. and Heimbarg, T. 2007. Defect formation of lytic peptides in lipid membranes and their influence on the thermodynamic properties of the pore environment. *Biochim. Biophys. Acta.* 1768:236-245.
- Osdol, VW., Biltonen, RL. and Johnson, ML. 1989. Measuring the kinetics of membrane phase transition. *J. Bioenerg. Biophys. Methods.* 20:1-46.
- Pawlak, M., Stankowski, S. and Schwarz, G. 1991. Melittin induced voltage-dependent conductance in DOPC lipid bilayers. *Biochim. Biophys. Acta.* 1062:94-102.
- Privalov, PL. 1980. Scanning microcalorimeters for studying macromolecules. *Pure Appl. Chem.* 52:479-497.
- Raghuraman, H. and Chattopadhyay, A. 2004. Interaction of melittin with membrane cholesterol: A fluorescence approach. *Biophys. J.* 87:2419-2432.
- Raghuraman, H. and Chattopadhyay, A. 2005. Cholesterol inhibits the lytic activity of melittin in erythrocytes. *Chem Phys Lipids.* 134:183-189.
- Rapaport, D., Peled, R., Nir, S. and Shai, Y. 1996. Reversible surface aggregation in pore formation by pardaxin. *Biophys. J.* 70:2502-2512.
- Raynor, RL., Zheng, B. and Kuo, JF. 1991. Membrane interactions of amphiphilic polypeptides mastoparan, melittin, polymyxin B, and cardiotoxin. Differential inhibition of protein kinase C, Ca²⁺/calmodulindependent protein kinase II and synaptosomal membrane Na,K-ATPase, and Na⁺ pump and differentiation of HL60 cells. *J. Biol. Chem.* 266:2753-2758.
- Rex, S. 1996. Pore formation induced by the peptide melittin in different lipid vesicle membranes. *Biophys. Chem.* 58:75-85.
- Rudenko, SV. and Patelaros, SV. 1995. Cation-sensitive pore formation in dehydrated erythrocytes. *Biochim Biophys Acta.* 1235:1-9.
- Sessa, G., Freer, JH., Colacicco, G. and Weissmann, G. 1969. Interaction of a lytic polypeptide, melittin, with lipid membrane systems. *J. Biol. Chem.* 244:3575-3582.

Schrader, W., Ebel, H., Grabitz, P., Hanke, E., Heimburg, T., Hoeckel, M., Kahle, M., Wente, F. and Kaatz, U. 2002. Compressibility of Lipid mixtures studied by calorimetry and ultrasonic velocity measurements. *J. Phys. Chem.* 106:6581-6586.

Stanley, HE. 1971. *Introduction to Phase Transitions and Critical Phenomena*. Oxford University Press, New York.

Stuehr, J. and Yeager, E. 1965. The Propagation of Sound in Electrolytic Solutions. In: *Physical Acoustics*. Ed. Mason, WP. (Vol. 2A). Academic Press, New York.

Terwilliger, T., Weissman, L. and Eisenberg, D. 1982. The structure of melittin in the form I crystals and its implication for melittin's lytic and surface activities, *Biophys. J.* 37:353-361.

Tosteson, MT. and Tosteson, TC. 1981. The sting. Melittin forms channels in lipid bilayers. *Biophys J.* 36:109-116.

Unger, T., Oren, Z. and Shai, Y. 2001. The effect of cyclization of magainin 2 and melittin analogues on the structure, function, and model membrane interactions: Implication to their mode of action. *Biochemistry.* 40:6388-6397.

Wilcox, W. and Eisenberg, D. 1992. Thermodynamics of melittin tetramerization determined by circular dichroism and implications for protein folding. *Protein Sci.* 1:641-653.

Wilson, AH. 1957. *Thermodynamics and statistical mechanics*. Cambridge University Press, Cambridge.

Winter, R., Gabke, A., Czeslik, C. and Pfeifer, P. 1999. Power-law fluctuations in phase-separated lipid membranes. *Phys. Rev. E.* 60:7354-7359.